

Raman investigation of amorphous carbon in diamond film treated by laser

Qihong Wu, Lin Yu, Yurong Ma, Yuan Liao, Rongchuan Fang et al.

Citation: *J. Appl. Phys.* **93**, 94 (2003); doi: 10.1063/1.1524306

View online: <http://dx.doi.org/10.1063/1.1524306>

View Table of Contents: <http://jap.aip.org/resource/1/JAPIAU/v93/i1>

Published by the [American Institute of Physics](#).

Related Articles

Large enhanced perpendicular magnetic anisotropy in CoFeB/MgO system with the typical Ta buffer replaced by an Hf layer

AIP Advances **2**, 032151 (2012)

Effect of adatom surface diffusivity on microstructure and intrinsic stress evolutions during Ag film growth

J. Appl. Phys. **112**, 043503 (2012)

Photoexpansion and nano-lenslet formation in amorphous As₂S₃ thin films by 800nm femtosecond laser irradiation

J. Appl. Phys. **112**, 033105 (2012)

Thickness effects on the magnetic and electrical transport properties of highly epitaxial LaBaCo₂O_{5.5+δ} thin films on MgO substrates

Appl. Phys. Lett. **101**, 021602 (2012)

Temperature dependence of nanometer-size metallic phase texture and its correlation with bulk magnetic and transport properties and defects of a (La_{0.4}Pr_{0.6})_{0.67}Ca_{0.33}MnO₃ film

Appl. Phys. Lett. **101**, 022404 (2012)

Additional information on J. Appl. Phys.


Journal Homepage: <http://jap.aip.org/>

Journal Information: http://jap.aip.org/about/about_the_journal

Top downloads: http://jap.aip.org/features/most_downloaded

Information for Authors: <http://jap.aip.org/authors>

ADVERTISEMENT



AIP Advances

Special Topic Section:
PHYSICS OF CANCER

Why cancer? Why physics? [View Articles Now](#)

Raman investigation of amorphous carbon in diamond film treated by laser

Qihong Wu, Lin Yu, Yurong Ma, Yuan Liao, and Rongchuan Fang^{a)}

Department of Physics, University of Science and Technology of China, Hefei, Anhui 230026, People's Republic of China

Ligong Zhang

Laboratory Of Excited State Processes, Changchun Institute of Optics Fine Mechanics and Physics, Changchun, Jilin 130021, People's Republic of China

Xiangli Chen and Kelvin Wang

GE Corporate Research and Development Center, 421 Hongcao Road, Shanghai 200233, People's Republic of China

(Received 22 May 2002; accepted 4 October 2002)

Micro-Raman spectroscopy was employed to investigate the structural changes of diamond films prepared by hot filament chemical vapor deposition and treated by femtosecond (fs) laser and nanosecond (ns) lasers. Breit–Wigner–Fano and Lorentzian line shape simulations were used to fit the spectra. For 266 nm ns laser treated samples, increasing laser power density results in the transformation of amorphous carbons in diamond films into nanocarbon clusters whose size increases and saturates rapidly at around 5.1 nm. At the same time, the Raman *G* peak position considerably shifts upwardly with increasing laser power density. The different change behavior of the nanocarbons and *G* peak is interpreted in light of the charge transfer from the graphite π bands to the localized edge states. As the 266 nm laser power density is high enough, a Raman peak in the range of 1150–1200 cm^{-1} appears, which is attributed to the presence of amorphous diamond. In the case of fs laser treated samples, much more power density ($>15 \text{ TW/cm}^2$) is needed to transform the amorphous carbon into nanocarbon phases. With increasing fs laser power density, the diamond peak is broadened and downshifted due to the presence of nanocrystalline diamond produced by the high laser power density. © 2003 American Institute of Physics. [DOI: 10.1063/1.1524306]

I. INTRODUCTION

It is well known that chemical vapor deposition (CVD) diamond films have become a desirable material for many applications such as heat sinks, optical windows, x-ray lithography masks, low-friction and wear resistant surfaces, and cutting tool coatings because of their excellent properties and the ease of the CVD growth method. However, CVD diamond films exhibit a polycrystalline structure with a great surface roughness and therefore the surface polishing techniques are time consuming and expensive due to the extreme hardness of the diamonds. Laser polishing (planarization) is a promising technique to diminish the roughness of the materials surface with some advantages such as contamination-free machining, precisely controlled removal rates, and the ability to remove material from a minuscule area. This method has been demonstrated for films of diamond,^{1–3} gallium nitride,⁴ silicon,⁵ and $(\text{Y}_{1-x}\text{Eu}_x)_2\text{O}_3$.⁶

It has been noticed that the excellent properties of diamond films are generally altered by structural defects, amorphous carbon, and/or other carbon phases produced by the laser treatment. The presence of structural defects and carbon phase formation can be characterized by Raman spectroscopy. To investigate the processes of laser-induced structural changes on the diamond surface is useful not only for a bet-

ter control of the quality of the laser-treated surface but also for a better understanding of the fundamental issues of laser interaction with materials.

Raman spectroscopy is sensitive to the change of translational symmetry and therefore to the characterization of crystalline, nanocrystalline, and amorphous carbons phases.^{7–13} In the disordered carbon films, normally there are two Raman peaks observed: the *G* peak around 1580–1600 cm^{-1} and the *D* peak around 1350 cm^{-1} , which are usually assigned to zone center phonons of $E_{(2g)}$ symmetry and *K*-point phonons of $A_{(1g)}$ symmetry, respectively.^{7,14–16} The *D* peak is activated by the relaxation of the $q=0$ selection rule,⁷ and its intensity is strictly connected to the presence of sixfold aromatic rings.¹⁷ On the other hand, sp^3 -coordinated carbon (single crystal diamond) has a narrow symmetric line in the Raman spectrum at 1332.5 cm^{-1} with the half width of about 1.7 cm^{-1} , which corresponds to the transverse optical phonon of the symmetry $T_{(2g)}$.

In this article, we present the results of Micro-Raman investigations of diamond films treated by ns and fs lasers. We found that the nanocarbon phases appear upon the short-pulsed laser treatments. The Raman line shapes and their evolution with experimental conditions are analyzed.

II. EXPERIMENT

Diamond films were prepared by the hot filament chemical vapor deposition (HFCVD) technique.¹⁸ The samples

^{a)} Author to whom correspondence should be addressed; electronic mail: fangrc@ustc.edu.cn

with grain sizes of about several tens of micrometers were treated in air by a Nd:yttrium–aluminum–garnet (YAG) ns laser (Spectra Physics) and a Ti:sapphire fs laser (Spectra Physics), respectively. The ns YAG laser was operated at the fourth harmonic wavelength of 266 nm with 8 ns pulse duration and up to 150 mJ/pulse at 10 Hz repetition rate. The fs laser was operated at 100 fs pulse width, 800 nm wavelength output, and up to 0.70 mJ/pulse at 1 kHz repetition rate. The divergence angles of these two lasers are all less than 0.5 mrad. A $\sim 100 \mu\text{m}$ diam focal spot was obtained by using a 200 mm focal-length quartz lens. In order to keep the temporal profile of the laser unchanged during the experiments, the laser output energy was kept at its maximum, and the distance between the lens and the sample was adjusted to get the proper energy density.

We use the symbols of ns266-L, ns266-M, and ns266-H to express samples treated by lower (52 GW/cm^2), middle (208 GW/cm^2), and higher (830 GW/cm^2) ns laser power densities, respectively, while fs800-L and fs800-H are the samples treated by lower (15 TW/cm^2) and higher (70 TW/cm^2) fs laser power densities, respectively. All the samples were treated for about 3 s. Micro-Raman spectroscopy was used to examine the alteration that occurred during the laser treatments of the diamond films. Raman spectra were taken in a near-backscattering geometry using a Labram-HR Micro-Raman spectrometer. The 514.5 nm line of an Ar^+ laser was the main excitation wavelength, and the 325 nm line of a He–Cd laser was also used to distinguish ordered and disordered carbons. The laser beam was focused to a $\sim 15 \mu\text{m}$ spot using a $50\times$ Olympus microscope objective, and a laser power of 1.5 mW was employed during the measurements. The spectra were taken in the range between 800 and 2000 cm^{-1} with a 1.8 cm^{-1} spectral resolution. In order to analyze the Raman spectra quantitatively, a Breit–Wigner–Fano (BWF) line + 2 Lorentzian lines + a linear line is employed to fit Raman spectra.^{19–21,17} The asymmetric BWF line shape, 2 Lorentzian lines shape, and linear line shape is fitted for the G peak, the D peak, the diamond (1332 cm^{-1}) peak, and the background, respectively. The BWF line shape is described as

$$I(\omega) = \frac{I_0(1 + 2(\omega - \omega_0)/Q\Gamma)^2}{1 + (2(\omega - \omega_0)/\Gamma)^2},$$

where $I(\omega)$ is the intensity as a function of frequency, I_0 is the peak intensity, ω_0 and Γ are the peak position and full width at half-maximum (FWHM), respectively, and $1/Q$ is the BWF coupling coefficient. The Lorentzian line shape is recovered in the limit $1/Q \rightarrow 0$. The G peak position, G peak FWHM ($\omega_{(G)}$), D peak position, D peak FWHM ($\omega_{(D)}$), diamond peak position, G peak FWHM ($\omega_{(\text{diamond})}$), and $I(D)/I(G)$ ratio obtained from the fittings to each spectrum are employed to quantify the changes which occurred in the various treated diamond films. The G peak position, maximum of the BWF line, is not at ω_0 but at lower frequencies

$$\omega_G = \omega_0 + \Gamma/2Q$$

as Q is negative. The $I(D)/I(G)$ is the ratio of the peak heights, not the peak areas because the information about the

breathing mode of the D peak is in the intensity maximum, not in the width which depends on the disorder.¹⁷

III. RESULTS

Figure 1 shows the Raman spectra of an as prepared diamond film (a), treated by 266 nm ns laser (b), (c), (d), and treated by 800 nm fs laser (e), (f) with different power densities. The components of the G peak, D peak, and diamond peak deduced from the fittings are also shown. The linear background has been subtracted and is not shown in the figures. Table I lists the data derived from the Fig. 1.

One can see from Fig. 1(d) and Table I that the diamond peak at 1332 cm^{-1} almost disappears and a new peak at 1192 cm^{-1} appears for samples treated by the highest 266 nm laser power density. We found that this new peak appeared typically in the range of $1150\text{--}1200 \text{ cm}^{-1}$ for different samples treated by the 266 nm laser with strong laser power density, e.g., 830 GW/cm^2 as in Fig. 1(d).

It also can be seen from Fig. 1 and Table I that with increasing laser power density in the case of 266 nm ns laser treatments, the diamond peak intensity decreases to almost zero in sample ns266-H but the peak position remains almost invariable; while the G peak shifts upward from 1539 to 1595 cm^{-1} and the FWHM narrows from 167 to 107 cm^{-1} , and the D peak saturates upwardly at 1357 cm^{-1} and the FWHM broadened first and then narrowed to 108 cm^{-1} . However, increasing laser power density in the case of 800 nm fs laser treatments, the diamond peak intensity decreases but retains a certain height even after 70 TW/cm^2 laser treatment, the diamond peak position shifts downwardly to 1328 cm^{-1} , and its corresponding FWHM broadened to 16.4 cm^{-1} ; the G peak shifts upward from 1539 to 1586 cm^{-1} and the FWHM narrows from 167 to 130 cm^{-1} , and the D peak shifts upward from 1322 to 1353 cm^{-1} and the FWHM broadened from 201 to 269 cm^{-1} .

Table II displays the G and D peak dispersions for samples treated by lasers derived from the Raman spectroscopy under 514.5 nm laser excitation (visible Raman spectra) and under 325 nm laser excitation (ultraviolet Raman spectra). The dispersion ΔG and ΔD are defined as the difference of the Raman shifts in the two measurements for the same samples. One can see from Table II that the D peak dispersion is much stronger than G peak except for sample fs800-L and for the untreated sample, and that both D and G peaks show strong dispersion for the untreated and the fs800-L sample.

IV. DISCUSSION

It has been shown that the dispersion behavior between the G and the D peaks is quite different. The G peak generated from the sp^2 C–C stretching vibrations does not disperse in graphite itself, nanocrystalline carbon, or glassy carbon,^{22–28} and it shows dispersion only in amorphous networks with a dispersion rate proportional to the degree of disorder,²⁹ due to a range of configurations with different local band gaps and different phonon modes. The dispersion of the D peak is strong in ordered carbon phases, and it shows a weak dispersion in amorphous carbon.²⁹ So, one can

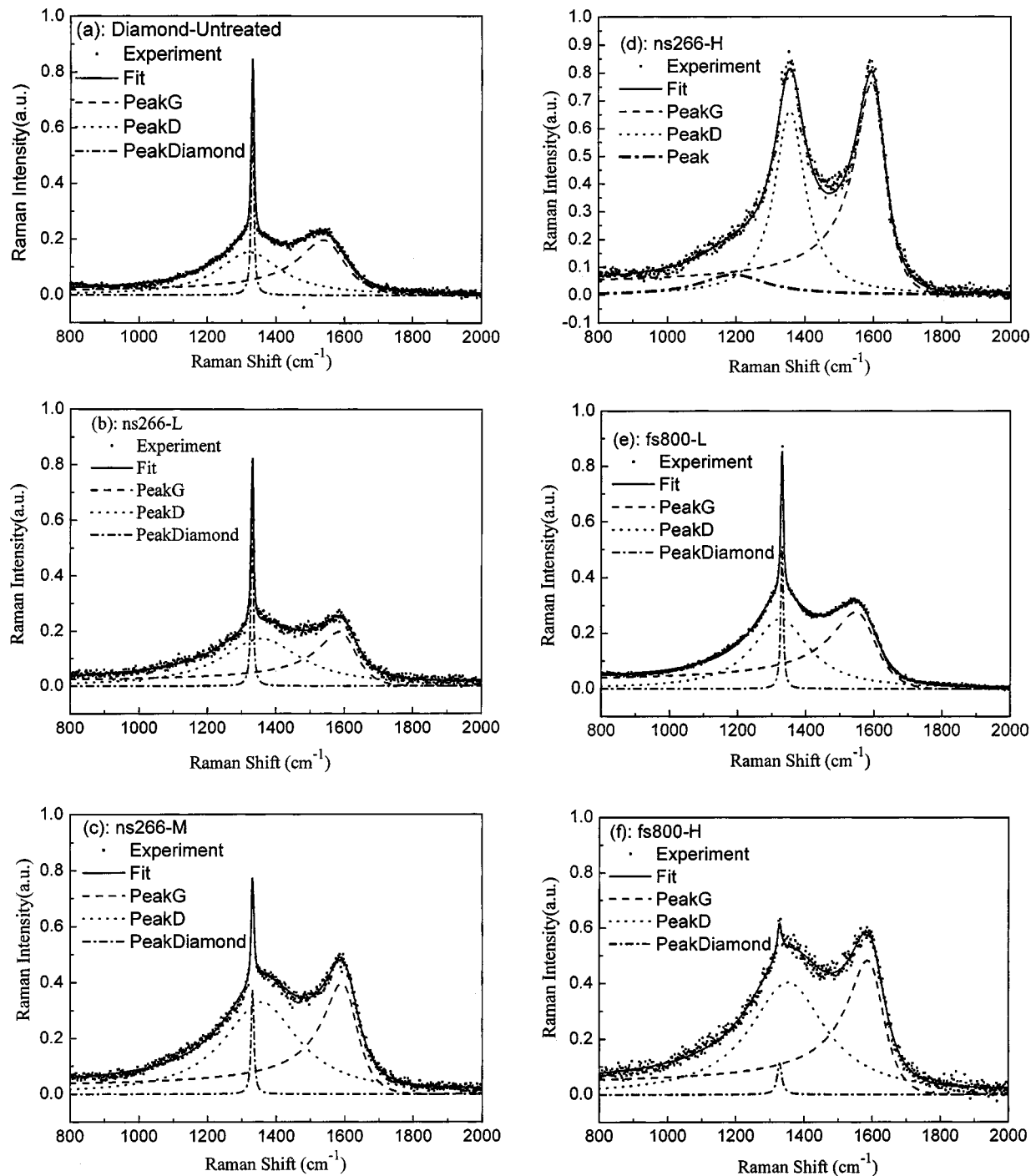


FIG. 1. Decomposition of Raman spectra of diamond films of: (a) an untreated sample, (b) 266 nm nanosecond laser treated sample with 52 GW/cm^2 ; (c) 266 nm nanosecond laser treated sample with 208 GW/cm^2 ; (d) 266 nm nanosecond laser treated sample with 830 GW/cm^2 ; (e) 800 nm femtosecond laser treated sample with 15 TW/cm^2 ; and (f) 800 nm femtosecond laser treated sample with 70 TW/cm^2 . The *G*, *D*, and diamond peak components resulting from the fit are also shown. The resulting fit is superimposed on the data. The linear background has been subtracted and is not shown. In (d) the diamond peak disappeared thoroughly and a new peak at $\sim 1192 \text{ cm}^{-1}$ appeared.

use this phenomenon to qualitatively distinguish the system order and disorder. From the data shown in Table II we can conclude that the carbon atoms in the untreated sample and sample fs800-L is a mixture of ordered carbons and amorphous carbons, and the content of disorder carbon in the other laser treated samples is very low. The peaks at 1322 and 1539 cm^{-1} in the untreated sample are *D* and *G* modes of amorphous carbon.^{30,31} The downshifted *G* peak of 1539

cm^{-1} and *D* peak of 1322 cm^{-1} of the untreated sample indicate the presence of bond-angle disorder and fourfold-coordinated bonds,³¹ which is consistent with the corresponding data in Table II. The narrowing in FWHM of the *G* *D* peaks with the increment of the laser power intensity in the 266 nm laser treated samples is the result from the removal of bond-angle disorder and the increasing order in amorphous carbons.

TABLE I. Results derived from measured micro-Raman spectra for samples treated by laser.

Sample	Diamond	ns266-L	ns266-M	ns266-H	fs800-L	fs800-H
Diamond	1331	1330	1331	—	1330	1328
$\omega_{(\text{Diamond})}$ (cm ⁻¹)	8.8	8.2	9.4	—	8.7	16.4
G (cm ⁻¹)	1539	1585	1591	1595	1546	1586
$\omega_{(G)}$ (cm ⁻¹)	167	136	123	107	160	130
D (cm ⁻¹)	1322	1357	1357	1357	1326	1353
$\omega_{(D)}$ (cm ⁻¹)	222	285	264	108	201	269
$I(D)/I(G)$	0.78	0.87	0.83	0.87	0.91	0.84

A. 266 nm ns laser treatment

Ferrari and Robertson¹⁷ proposed a phenomenological three-stage model to describe the character of G and D peaks in visible Raman spectroscopy for *amorphization* of graphite→nanocrystalline graphite (stage 1), nanocrystalline graphite→amorphous carbon (stage 2), and amorphous carbon→tetrahedron carbon (stage 3). As discussed above, the carbon phases in 266 nm ns laser treated samples are mainly ordered carbons, therefore it is suitable to discuss our Raman spectra using the three-stage model. According to this model, the untreated samples should be in stage 2 and the 266 nm laser treated samples in stage 1, i.e., the amorphous carbon, has been graphitized and changed into nanocrystalline graphite after the 266 nm ns laser treatment. In our BWF+Lorentzian fitting, the fit of the D peak is the least accurate, because it is only a low frequency shoulder of the G peak. Thus, from Table I, it is reasonable to assume that the ratio of $I(D)/I(G)$ of the three 266 nm laser treated samples is nearly the same although the ratio $I(D)/I(G) = 0.83$ for sample ns266-M, and 0.87 for the other two samples. There are two factors responsible for the shift of the D peak. First, smaller aromatic clusters have higher modes and upshift the D peak position.³² Second, a decrease in number of ordered aromatic rings on passing from nanocrystalline graphite to amorphous carbon lowers D and reduces its intensity, due to the softening of the vibrational density of states (VDOS).³³ Tuinstra and Koenig⁷ found that the Raman intensity of the $I(D)/I(G)$ is inversely proportional to the cluster diameter La

$$I(D)/I(G) = C(\lambda)/La,$$

where $C(514.5 \text{ nm}) \sim 4.4 \text{ nm}^{34}$ and La is called in-plane correlation length. The ratio $I(D)/I(G)$ and the D peak of the 266 nm laser treated samples remain almost constant, indi-

cating that La increased and saturated sharply at a value of $\sim 5.1 \text{ nm}$ after the 266 nm laser treatment. Note that the Tuinstra–Koenig (TK) equation will underestimate La due to the dominant effect of small crystallites compared with the value obtained by x-ray diffraction.³⁵ According to the three-stage model, the G peak should not upshift with increasing 266 nm laser power density, which is contrary to our experiment. This discrepancy can be explained by the charge-transfer effect related to the edge states of nanocrystalline carbon.³⁶

There are two factors responsible for the upshift of the G peak in nanocarbons: (a) the decrease of La of nanocrystalline carbons,^{15,16} and (b) the charge-transfer effect related to the edge states. The decrease of La can be ruled out as the La remains almost constant as derived from the D peak position and the ratio of $I(D)/I(G)$. The charge-transfer effect seems to be the possible mechanism capable of upshifting the G peak to the extent that we observe. Theoretical reports^{37,38} suggest that finite graphite systems having a zigzag edge exhibit a special edge state, which will be easily formed in nanocarbon because only three or four zigzag sites per sequence are enough to show an edge state in the graphene ribbons. The corresponding energy bands are almost flat at the Fermi level (near the contact point of the π – π^* levels of nanographite) and thereby give a sharp peak in the density of states. The charge density in the edge state is strongly localized on the zigzag edge sites. Nanocarbon phases with different size will broaden the energy level of π band and the edge-state band, consequently these bands may overlap, so that the bottom of the edge-state band is lower than the top of the graphite π band. Thus it is possible that there is a charge transfer from the graphite π band to these edge states, where the edge states act as acceptors. This conjecture is justified by experimental evidence about the presence of

TABLE II. G peak and D peak dispersion for samples treated by laser derived from visible Raman spectra and ultraviolet Raman spectra.

		Diamond	ns266-L	ns266-M	ns266-H	fs800-L	fs800-H
Visible (514.5 nm)	G (cm ⁻¹)	1539	1585	1591	1595	1546	1586
	D (cm ⁻¹)	1322	1357	1357	1357	1326	1353
Ultraviolet (325 nm)	G (cm ⁻¹)	1560	1587	1593	1598	1598	1589
	D (cm ⁻¹)	1353	1420	1413	1424	1376	1404
Shift	ΔG (cm ⁻¹)	21	2	2	3	52	3
	ΔD (cm ⁻¹)	31	63	56	67	50	51

holes in nanographite materials.³⁹ This charge transfer from the graphite π bands to the edge states would lead to a stiffening of the C–C bonds in the plane, thus leading to the upshift of the G peak position. Therefore, it is easy to produce the zigzag structure in nanocarbon phases after the 266 nm ns laser treatment, which will produce a charge-transfer effect. The laser induced charge-transfer effect is also verified in nanocarbon films prepared by HFCVD as shown in Fig. 2.

As shown in Fig. 1(d), the diamond peak almost disappears for sample ns266-H. To fit the whole spectrum another new band (Lorentzian) near 1192 cm^{-1} should be taken into account. This new Raman peak only appears in samples treated by a strong laser power. The peak positions are located in the $1150\text{--}1200\text{ cm}^{-1}$ spectral range depending on the laser power density and the fitting procedures, because the peak intensity is very weak.

A peak near 1150 cm^{-1} in the visible Raman can always be observed in the poor quality CVD diamond. Nemanich *et al.*⁴⁰ proposed that this peak could be the result of nanocrystalline or amorphous diamond, a precursor structure of diamond. A small grain size would be expected to relax the $q=0$ selection rule and allow phonon modes with $q\neq 0$ to contribute. Other workers also supported this assignment.^{10,41–45} But Ferrari and Robertson⁴⁶ argued that this peak should not be assigned to nanocrystalline diamond or other sp^3 -bonded phases, they assigned this peak to transpolyacetylene segments at grain boundaries and surfaces, which is clearly connected with the presence of hydrogen, and the peak of transpolyacetylene segments can be weakened by postdeposition annealing. In our case, the hydrogen content in diamond film is very low as derived from the ratio between the slope m of the fitted linear background and the intensity of the G peak $m/I(G)$, which is near zero ($m/I(G)\sim 1.0\times 10^{-6}$ for all samples),⁴⁷ and this new Raman peak only appeared in the sample ns266-H. However it is impossible that the hydrogen content in sample ns266-H is higher than that of the untreated samples because of the thermal effect of the laser treatment, which can be as high as several thousand degrees Centigrade according to the thermal vaporization model.^{48,49} This is contrary to the previous result of Ferrari and Robertson. Therefore it is impossible to relate the $\sim 1190\text{ cm}^{-1}$ Raman peak to the origin of a transpolyacetylene segments proposed by Ferrari and Robertson.⁴⁶

In order to further explore the origin of the $\sim 1192\text{ cm}^{-1}$ peak, nanocrystal carbon (NC) film prepared by HFCVD was also treated by a 266 nm ns laser. The visible Raman spectra (514.5 nm) of NC film before and after laser treatment are shown in Fig. 2. The NC film shows two sharp peaks, i.e., the G and D peaks, and an additional peak at 1172 cm^{-1} can also be clearly observed. After laser treatment, the treated NC 266 nm sample shows two additional peaks at 1217 and 1274 cm^{-1} , and the 1172 cm^{-1} peak is enhanced and narrowed by the 266 nm ns laser treatment. This indicates that the 1172 cm^{-1} peak cannot be attributed to the presence of a transpolyacetylene segment, if we consider the thermal effect of 266 nm laser treatment. Figure 3 shows the VDOS of diamond,⁵⁰ where there is a maximum peak at 1260 cm^{-1}

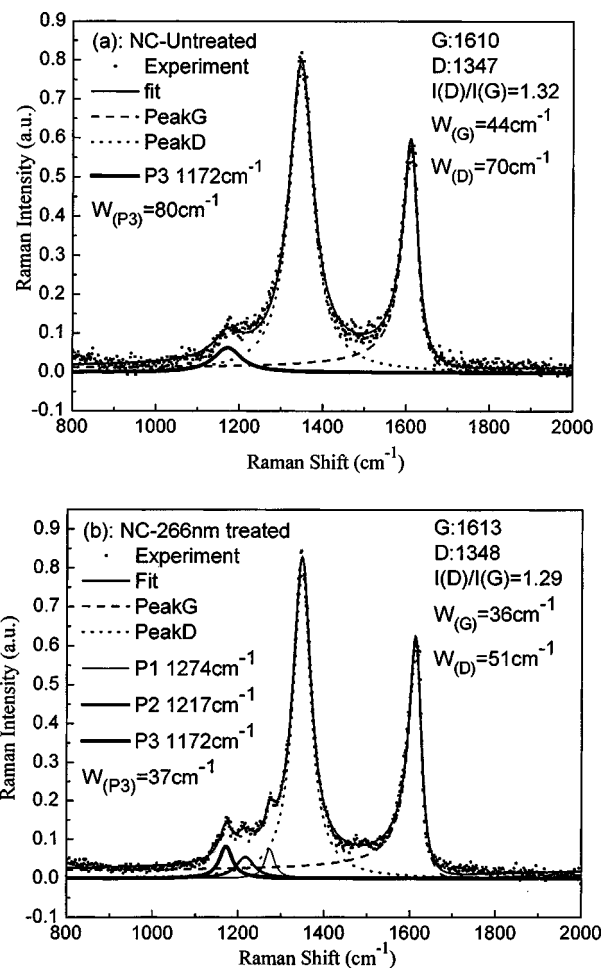


FIG. 2. Decomposition of Raman spectra of CVD nanocarbon films of: (a) an untreated sample and (b) 266 nm nanosecond laser treated sample. The G , D , $P1$, $P2$, and $P3$ peak components resulting from the fit are also shown. The resulting fit is superimposed on the data. The linear background has been subtracted and not shown. The results of peak position and FWHM of D and G peak, and height ratio of $I(D)/I(G)$ are also shown.

and a kink at 1175 cm^{-1} , which are equal roughly to the peaks at 1274 and 1172 cm^{-1} . Thus we attribute the peaks at 1274 and 1172 cm^{-1} to the presence of amorphous diamond as proposed by Nemanich *et al.*⁴⁰ Therefore we attribute the new peak at $\sim 1192\text{ cm}^{-1}$ in sample ns266-H to amorphous diamond after 266 nm ns laser treatment.

B. 800 nm fs laser treatment

Sample fs800-L is in stage 2 in the three-stage model as well as the untreated sample, while sample fs800-H is in stage 1. Therefore, it is meaningful to compare sample fs800-L with the untreated sample. The upshift of the G peak position and the increase of $I(D)/I(G)$ after the 800 nm fs laser treatment indicate that the decrease of sp^3 content, i.e., the number of aromatic rings order increase and the bond-angle disorder decrease, therefore the D peak position increase³³ and the FWHM of the G and D peaks narrows.

Generally, as the laser power intensity increases, more amorphous carbon phases in the diamond film can change into nanocarbon phases because of a more serious thermal effect. In the ns laser treatment, the 52 MW/cm^2 power in-

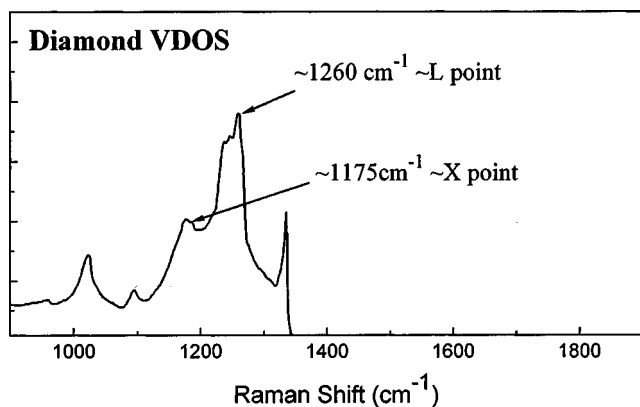


FIG. 3. The vibrational density of states of diamond from Ref. 48. The maximum peak at 1260 cm^{-1} and a kink at 1175 cm^{-1} are also shown.

tensity is enough to transform the amorphous carbon into nanocarbon material, while in the fs laser treatment, a laser power intensity greater than 15 TW/cm^2 is needed. This is because the thermal effect is much more serious in ns laser treatment than that of the fs laser treatment.

In sample fs800-H, the diamond peak position is broadened and downshifted obviously. There are three factors responsible for the broadening and downshift of the peaks of the diamond film: (a) defects produced by the laser treatment, (b) tensile stress in the diamond film, and (c) nanocrystal diamond produced by the laser treatment. Photochemically generated defects can usually be found in fs laser treatments of dielectrics such as barium aluminum borosilicate glass,⁵¹ fused silica,⁵² and diamond.⁵³ During the fs laser treatment of diamond, the defects can introduce an sp^2 bond disorder into the sp^3 -bond dominated system (diamond). Thus the diamond bands can be broadened by the disorder or diminished phonon lifetimes resulting from defects. But the broadening and downshift of the diamond peak in the fs800-H sample should not be due to the defects effect because there is no such broadening and downshift in the ns laser treated samples and the lower intensity laser treated sample fs800-L. The tensile stress effect can also be ruled out because the thermal effect during fs laser treatment is small and there is no obvious change of the diamond peak in samples treated by the 266 nm ns laser in which thermal effects should be larger than sample fs800-H. Therefore, the only mechanism capable of broadening and downshifting the diamond peak to the extent that we observe is the presence of nanocrystalline diamond produced by the fs laser treatment.

It is possible to rapidly heat the condensed material to temperatures far above the critical temperature by a high power subpicosecond laser.⁵⁴ This phenomenon has been verified by recent experiments.^{55–57} Thus, it is possible to heat the nanocrystalline carbon in sample fs800-H to above the critical temperature ($>4500\text{ K}$) by the 800 nm fs laser. During the treatment of sample fs800-H, the laser power intensity is so large (70 TW/cm^2) that the shock wave produced by the laser treatment can be very high. If the shock wave pressure is higher than several tens of GP, the instant condition is very similar to that of ultradisperse diamond preparation by the detonation technique. Therefore, it is pos-

sible to produce nanocrystal diamond in sample fs800-H by a high power fs laser exposure. In other samples, although the temperature may be sufficiently elevated, the instant shock wave pressure is not high enough to produce nanocrystal diamond from the nanocarbon material.

The size of nanocrystalline diamond in sample fs800-H derived from the FWHM and peak position of diamond peak is about 5–6 nm,⁵⁸ which is consistent with the size of nanocarbon (5.2 nm) derived from TK equation.⁷ This also indicates that the nanocrystal diamond maybe transformed from the nanocarbon phase in sample fs800-H.

V. CONCLUSION

The transformation of amorphous carbon to nanocarbon in diamond film treated by ns and fs lasers has been investigated by Micro-Raman spectroscopy. The line shape of Raman spectra and the evolution with experimental conditions have been analyzed. With increasing 266 nm laser power intensity, the charge-transfer effect related to the edge states of the nanocarbon phase is used to explain the upshift of the *G* peak position, and the peak in the range of $1150\text{--}1200\text{ cm}^{-1}$ is attributed to amorphous diamond. In the case of the 800 nm fs laser treatment, the downshift and broadening of the diamond peak in sample fs800-H is due to the presence of nanocrystalline diamond produced by the ultrahigh intensity laser treatment.

ACKNOWLEDGMENTS

The authors would like to thank B. Miao for assistance of ns laser operation, H. Jin, and H. Y. Xu for assistance with fs laser operation, and Y. Q. Dong for providing nanocarbon film.

- ¹P. Tosin, W. Luthy, and H. P. Weber, *Phys. Bl.* **52**, 569 (1996).
- ²S. M. Pimenov, A. A. Smolin, V. G. Ralchenko, and V. I. Konov, *Diamond Films Technol.* **5**, 141 (1994).
- ³R. Windholz and P. A. Molian, *J. Mater. Sci.* **32**, 4295 (1997).
- ⁴T. Akane, K. Sugioka, H. Ogino, H. Takai, and K. Midorikawa, *Appl. Surf. Sci.* **148**, 133 (1999).
- ⁵M. Jyumonji, K. Sugioka, H. Takai, and K. Toyoda, *Jpn. J. Appl. Phys., Part 1* **34**, 6878 (1995).
- ⁶J. Mckittrick *et al.*, *J. Mater. Res.* **13**, 3019 (1998).
- ⁷F. Tuinstra and J. L. Koenig, *J. Chem. Phys.* **53**, 1126 (1970).
- ⁸S. R. Salis, D. J. Gardiner, M. Bowden, J. Savage, and D. Rodway, *Diamond Relat. Mater.* **5**, 589 (1996).
- ⁹M. Yoshikawa, N. Nagai, M. Matsuki, H. Fukuda, G. Katagiri, H. Ishida, A. Ishitani, and I. Nagai, *Phys. Rev. B* **46**, 7169 (1992).
- ¹⁰J. Wagner, M. Ramsteiner, C. Wild, and P. Koidl, *Phys. Rev. B* **40**, 1817 (1989).
- ¹¹M. A. Tamor, J. A. Haire, C. H. Wu, and K. C. Hass, *Appl. Phys. Lett.* **54**, 123 (1989).
- ¹²M. A. Tamor and W. C. Vassel, *J. Appl. Phys.* **76**, 3823 (1994).
- ¹³J. Schwan, S. Ulrich, V. Bathori, H. Erhardt, and S. R. P. Silva, *J. Appl. Phys.* **80**, 440 (1996).
- ¹⁴R. J. Nemanich and S. A. Solin, *Phys. Rev. B* **20**, 392 (1979).
- ¹⁵P. Lespade, R. Al-Jishi, and M. S. Dresselhaus, *Carbon* **20**, 427 (1982).
- ¹⁶P. Lespade, A. Marchard, M. Couzi, and F. Cruege, *Carbon* **22**, 375 (1984).
- ¹⁷A. C. Ferrari and J. Robertson, *Phys. Rev. B* **61**, 14095 (2000).
- ¹⁸Y. Liao, C. H. Li, Z. Y. Ye, C. Chang, G. Z. Wang, and R. C. Fang, *Diamond Relat. Mater.* **9**, 1716 (2000).
- ¹⁹D. G. McCulloch, S. Praver, and A. Hoffman, *Phys. Rev. B* **50**, 5905 (1994).
- ²⁰D. G. McCulloch and S. Praver, *J. Appl. Phys.* **78**, 3040 (1995).

- ²¹S. Praver, K. W. Nugent, Y. Lifshitz, G. D. Lempert, E. Grossman, J. Kulik, I. Avigal, and R. Kalish, *Diamond Relat. Mater.* **5**, 433 (1996).
- ²²R. P. Vidano, D. B. Fishbach, L. J. Willis, and T. M. Loehr, *Solid State Commun.* **39**, 341 (1981).
- ²³Y. Kawashima and G. Katagiri, *Phys. Rev. B* **52**, 10 053 (1995).
- ²⁴Z. Wang, X. Huang, R. Xue, and L. Chen, *J. Appl. Phys.* **84**, 227 (1998).
- ²⁵Y. Wang, D. C. Alsmeyer, and R. L. McCreery, *Chem. Mater.* **2**, 557 (1990).
- ²⁶I. Pocsik, M. Koos, M. Hundhausen, and L. Ley, in *Amorphous Carbon: State of the Art*, edited by S. R. P. Silva *et al.* (World Scientific, Singapore, 1998), p. 224.
- ²⁷K. Sinha and J. Menendez, *Phys. Rev. B* **41**, 10845 (1990).
- ²⁸P. Tan, Y. Deng, and Q. Zhao, *Phys. Rev. B* **58**, 5435 (1998).
- ²⁹A. C. Ferrari and J. Robertson, *Phys. Rev. B* **64**, 75414 (2001).
- ³⁰D. S. Knight and W. B. White, *J. Mater. Res.* **4**, 385 (1989).
- ³¹R. O. Dillon, J. A. Woollam, and V. Katkanant, *Phys. Rev. B* **29**, 3482 (1984).
- ³²C. Mapelli, C. Castiglioni, G. Zerbi, and K. Mullen, *Phys. Rev. B* **60**, 12710 (1999).
- ³³D. Beeman, J. Silverman, R. Lynds, and M. R. Anderson, *Phys. Rev. B* **30**, 870 (1984).
- ³⁴M. J. Matthews, M. A. Pimenta, G. Dresselhaus, M. S. Dresselhaus, and M. Endo, *Phys. Rev. B* **59**, 6585 (1999).
- ³⁵H. Wilhem, M. Lelaurain, E. McRae, and B. Humbert, *J. Appl. Phys.* **84**, 6552 (1998).
- ³⁶B. L. V. Prasad, H. Sato, T. Enoki, Y. Hishiyama, Y. Kaburagi, A. M. Rao, P. C. Eklund, K. Oshida, and M. Endo, *Phys. Rev. B* **62**, 11209 (2000).
- ³⁷M. Fujita, K. Wakabayashi, K. Nakada, and K. Kusakabe, *J. Chem. Phys.* **65**, 1920 (1996).
- ³⁸K. Nakada, M. Fujita, G. Dresselhaus, and M. S. Dresselhaus, *Phys. Rev. B* **54**, 17954 (1996).
- ³⁹Y. Shibayama, H. Sato, T. Enoki, X. X. Bi, M. S. Dresselhaus, and M. Endo, *J. Photogr. Sci.* **69**, 734 (2000).
- ⁴⁰R. J. Nemanich, J. T. Glass, G. Lucovsky, and R. E. Shroder, *J. Vac. Sci. Technol. A* **6**, 1783 (1988); R. E. Shroder, R. J. Nemanich, and J. T. Glass, *Phys. Rev. B* **41**, 3738 (1990).
- ⁴¹K. Kobashi, K. Nishimura, Y. Kawate, and T. Horiuchi, *Phys. Rev. B* **38**, 4067 (1988).
- ⁴²E. D. Obratzsova, V. L. Kuznetsov, E. N. Loubnin, S. M. Pimenov, and V. G. Pereverzev, in *Nanoparticles in Solids and Solutions*, edited by J. H. Fendler and I. Dekany (Kluwer, Dordrecht, 1996).
- ⁴³M. Nishitani-Gamo, T. Ando, K. Yamamoto, K. Watanabe, P. A. Denning, Y. Sato, and M. Sekita, *Appl. Phys. Lett.* **70**, 1530 (1997).
- ⁴⁴J. Wagner, C. Wild, and P. Koidl, *Appl. Phys. Lett.* **59**, 779 (1991).
- ⁴⁵K. Okada, H. Kanda, S. Komatsu, and S. Matsumoto, *J. Appl. Phys.* **88**, 1674 (2000).
- ⁴⁶A. C. Ferrari and J. Robertson, *Phys. Rev. B* **63**, 121405 (2001).
- ⁴⁷B. Marchon, J. Gui, K. Grannen, G. C. Rauch, J. W. Ager, S. R. P. Silva, and J. Robertson, *IEEE Trans. Magn.* **33**, 3148 (1997).
- ⁴⁸A. Miotello and R. Kelly, *Appl. Phys. Lett.* **67**, 3535 (1995).
- ⁴⁹J. J. Chang and B. E. Warner, *Appl. Phys. Lett.* **69**, 473 (1996).
- ⁵⁰P. Pavone, K. Karch, O. Shutt, W. Windl, D. Strauch, P. Giannozzi, and S. Baroni, *Phys. Rev. B* **48**, 3164 (1993).
- ⁵¹W. Kautek and J. Kruger, *Appl. Phys. Lett.* **69**, 3146 (1996).
- ⁵²M. Lenzner, J. Krüger, W. Kautek, and F. Krausz, *Appl. Phys. A: Mater. Sci. Process.* **69**, 465 (1999).
- ⁵³G. Dumitru, V. Romano, H. P. Weber, M. Sentis, and W. Marine, *Appl. Phys. A: Mater. Sci. Process.* **74**, 729 (2002).
- ⁵⁴N. A. Inogamov, Yu. V. Petrov, S. I. Anisimov, A. M. Oparin, N. V. Shaposhnikov, D. von der Linde, and J. Meyer-ter-Vehn, *JETP Lett.* **69**, 310 (1999).
- ⁵⁵D. von der Linde, K. Sokolowski-Tinten, and J. Bialkowski, *Appl. Surf. Sci.* **109/110**, 1 (1996).
- ⁵⁶K. Sokolowski-Tinten *et al.*, *Phys. Rev. Lett.* **81**, 224 (1998).
- ⁵⁷K. Sokolowski-Tinten *et al.*, *Proc. SPIE* **3343**, 46 (1998).
- ⁵⁸A. E. Aleksenski, M. V. Badakova, A. Ya. Vul, V. Yu. Davydov, and Yu. A. Pevtsova, *Phys. Solid State* **39**, 1007 (1997).